



Research article

Boron supply maintains efficient antioxidant system, cell wall components and reduces aluminum concentration in roots of trifoliate orange



Muhammad Riaz^a, Lei Yan^a, Xiuwen Wu^a, Saddam Hussain^b, Omar Aziz^a, Cuncang Jiang^{a,*}

^a Microelement Research Center, College of Resources and Environment, Huazhong Agricultural University, Wuhan, Hubei, 430070, PR China

^b Department of Agronomy, University of Agriculture Faisalabad, 38040, Punjab, Pakistan

ARTICLE INFO

Keywords:

Boron
Aluminum toxicity
Cell wall components
Lumogallion
Confocal microscopy

ABSTRACT

Aluminum (Al) toxicity in the acid soils (pH ≤ 5) is the major limiting abiotic factor affecting the productivity of crops. Boron (B) has been reported to alleviate Al toxicity. In spite of recent advances, it is not clear how B relieves Al toxicity. Results demonstrated that Al toxicity hampered the root elongation. Moreover, lumogallion fluorescent molecular probe unequivocally localized mostly bound Al to the periphery of the cell wall (CW) and to the nuclei. Additionally, Al toxicity induced variations in the CW components through the accumulation of pectin and hemicellulose. Nevertheless, B supply reduced callose deposition, increased root growth and reduced changes in the CW components under Al toxicity. Moreover, B supply reduced the un-methylated pectin while increased the degree of methyl esterification of pectin. These results imply that B due to its role in the CW formation could reduce aluminum-induced negative effects on plant growth by attenuating apoplastic Al³⁺ and changes in the CW components which ultimately results in the improved root growth.

1. Introduction

Aluminum toxicity is a major limitation in the development and production of high-quality crops on acidic soils. More than 50% soils of the world are acidic and mostly existed in tropical and subtropical regions of the world (Uexküll and Mutert, 1995). Aluminum is the third most abundant element in the earth crust, and fortunately, it is present as insoluble harmless oxides and aluminosilicates (Poschenrieder et al., 2008). However, the decline in soil pH due to environmental and/or anthropogenic factors enhances the transformation of Al to soluble Al³⁺, which is a highly phytotoxic and a major threat to plant productivity. The most observable effect of aluminum is on the plant root growth through inhibiting its growth (Kochian et al., 2004). The aluminum-induced effects on roots occur within a short span of time. Even small quality of aluminum has been reported to restrict the root elongation in a number of aluminum sensitive plant species (Llugany et al., 1995). The mechanism(s) underlying the cause of hindrance of root elongation is a matter of great concern. Several convincing reports advocated that the root apex is a major site of aluminum toxicity (Kochian et al., 2004). In addition, aluminum toxicity mechanisms are likely to be functioning in the apoplast, symplast and the plasma membrane (Sivaguru and Horst, 1998; Horst et al., 2010). The root development depends on cell division as well as cell elongation in the growing regions (Jones et al., 2006). It is also believed that disruption

of cell elongation as well as cell division, is the potent reason of inhibition of root elongation, but disruption of cell elongation is widely accepted mechanism for the hindrance of root growth (Kollmeier et al., 2000) along with several other operational mechanisms that are influenced by Al exposure (Lazof and Holland, 1999). Aluminum is adsorbed to the apoplast and this binding is likely to be responsible for limiting root growth (Chang et al., 1999). The bound apoplastic Al may induce alterations in the cell wall (CW) constituents (Ma et al., 2004). It has long been reported that Al also binds to the dsDNA and nuclei of the cells (Tice et al., 1992). However, it is still questionable which part of dsDNA provides sites for Al binding after entering the symplasm.

Boron (B) is an indispensable nutrient for higher plants including citrus (Loomis and Durst, 1992). The B deficiency and aluminum toxicity exhibit same symptom of disorders on roots through inhibiting root elongation (Lenoble et al., 1996b; Wu et al., 2017; Yan et al., 2018). The B defines the CW structure and ensures its stability under harsh condition of environment. The CW of higher plants contains a large amount of polysaccharides including rhamnogalacturonan (RG-II) and B aids in the cross-linking of RG-II together through diester bonds (O'Neill et al., 2001). The stable and well-packed network of cells develops stable CW with reduced pore sizes (Fleischer et al., 1999). It also tightens CW that restricts entry of large molecules/elements into the cell. The CW of plant plays a key role in aluminum toxicity as it is the main site of aluminum accumulation and subsequently toxicity in plants

* Corresponding author.

E-mail address: jcc2000@mail.hzau.edu.cn (C. Jiang).

<https://doi.org/10.1016/j.plaphy.2019.02.003>

Received 19 November 2018; Received in revised form 7 February 2019; Accepted 7 February 2019

Available online 08 February 2019

0981-9428/ © 2019 Elsevier Masson SAS. All rights reserved.

(Horst et al., 2010). Moreover, the binding of aluminum to the CW is detrimental to the plants in performing normal functions, and this bound CW Al may decrease elasticity and viscosity of membranes (Ma et al., 2004). Therefore, it is logical to speculate that the CW has an important role to hinder toxic aluminum. The primary CW with its carboxylate group has been reported the major pool of Al adsorption (Chang et al., 1999; Taylor et al., 2000).

China is one of the main producers of citrus in the world. The trifoliolate is well-known rootstock of citrus in China. Most of the citrus producing regions in the world are located in acidic regions with $\text{pH} \leq 5$. The citrus in Jiangxi (82.1% acid soil) is prone to aluminum toxicity and B deficiency due to leaching of B through the root zone and declining pH, that ultimately resulted in the poor quality of fruit and productivity (Han et al., 2008). Although, soil acidity can be managed by liming, nevertheless, this method is costly, laborious and time-consuming (Alva et al., 1986). Therefore, it is inevitable to identify alternative methods that can be socially adopted and economically feasible. Boron has been reported to enhance tolerance against toxic aluminum and has been reported to alleviate aluminum toxicity in many plants. (Lenoble et al., 1996a; Lenoble et al., 1996b; Li et al., 2017). Therefore, the present attempt was made to explore the role of supplementary boron beyond the optimum need of citrus in mitigating aluminum toxicity by observing apoplastic Al^{3+} fractions through confocal laser microscopy and callose deposition, moreover, to study how B could induce antioxidant enzyme system in order to alleviate aluminum-induced root damage and changes in root cell wall components.

2. Material and methods

2.1. Growth condition, plant material, and experimental treatments

The present study was conducted on trifoliolate orange. The seeds of trifoliolate were grown under control conditions, and after germination, uniform seedlings were transplanted to 8 L pots at Huazhong Agriculture University, Wuhan, China. The nutrient solution was applied as follows: 2 mM KNO_3 , 0.50 mM MgSO_4 , 1.23 mM $\text{Ca}(\text{NO}_3)_2$, 0.10 mM K_2HPO_4 , 4.45 μM MnCl_2 , 0.8 μM $\text{ZnSO}_4 \cdot 7\text{H}_2\text{O}$, 0.18 μM Na_2MoO_4 , 13 μM Fe-EDTA and 0.16 μM CuSO_4 . The solution pH was regularly monitored and maintained at 4.2 ± 0.2 by means of 0.1 M HCl. The aeration was supplied with an aeration system for 20 min after every 4 h intervals. The hydroponic solution was renewed every after 3 days. Al activity was calculated with a computer-based software GeoChem-PC v1.0. High-quality analytical grade salts were used to prepare reagents. The experiment had a complete randomized design with six treatments and each treatment was replicated three times. The B (0, 10 and 30 μM as H_3BO_3) and Al (0 and 200 μM as $\text{AlCl}_3 \cdot 6\text{H}_2\text{O}$) were applied to seedlings for 10 weeks. For easy understanding of the study results, the treatments were denoted as B_0Al - (0 μM B + 0 μM Al), $\text{B}_0\text{Al}+$ (0 μM B + 200 μM Al), B_1Al - (10 μM B + 0 μM Al), $\text{B}_1\text{Al}+$ (10 μM B + 200 μM Al), B_2Al - (30 μM B + 0 μM Al) and $\text{B}_2\text{Al}+$ (30 μM B + 200 μM Al). The B_1Al - treatment was considered as control.

2.2. Plant sampling and specimen preparation

The seedlings after growing in the culture solution for 10 weeks were removed from the pots and washed with ultra-pure water. The root apices from the primary roots (0–1 cm) were excised and subjected to microscopic observations. The excised root tips were sliced into thin sections suitable for the confocal laser microscopy. The root segments were rinsed with 10 mM citrate for 15 min at 25 °C and then stained with Al specific dye lumogallion in dark at 45 °C for 1 h with constant shaking at $180 \times g$. The stained roots were fixed on the microscopic glass slides and stained with DAPI (Silva et al., 2000). The solutions of (10 μM) lumogallion and (1 $\mu\text{g}/\text{mL}$) DAPI were prepared in dark conditions and preserved at 4 °C following the manufacturers' guidelines. The lumogallion fluorimetric reagent ($\text{C}_{12}\text{H}_9\text{ClN}_2\text{O}_6\text{S}$) was purchased

from Tokyo Chemical Industries, Japan, and DAPI from Beyotime biotechnology.

The confocal laser fluorescence microscope (Olympus IX81) was used to observe the root samples. DAPI was imaged at around 460 nm, and to visualize Al- lumogallion complex, emitted fluorescence was collected at wavelengths from 500 to 550 nm.

Through consecutive scanning, the noise was minimized and the specimen was scanned at least 3 times at XY planes and 1024×1024 pixels, and finally transferred to Adobe Photoshop CS5.

2.3. Extraction of cell wall material

The root tips (0–10 mm, 100 roots/replication) were excised and processed for the extraction of cell wall. The roots were homogenized into liquid nitrogen. The homogenate was washed with ice cold water (once) and 80% ethanol (thrice) and centrifuged at $5000 \times g$ for 10 min. The resultant residue was again washed with a mixture of methanol: chloroform (v/v, 1:1) and acetone (once) and re-centrifuged as described by Wu et al. (2017). The insoluble filtrate was used for the determination of B and Al.

2.4. Measurement of aluminum and boron concentration in roots

The citrate washed root tips (0–1 cm) were excised from seedlings that were grown under different concentrations of B and Al for 10 weeks. Following by rinsing with (10 mM) citrate, the root tips were relocated to teflon tubes containing 1.2 mL of 2 M HNO_3 (prepared from 80% HNO_3) and incubated at 30 °C for 24 h in a horizontal shaker with constant stirring. Subsequently, the sample was diluted and determined by graphite furnace atomic absorption spectrophotometer. The same procedure was carried out with freeze-dried crude cell wall for the measurement of Al. The citrate solution collected during rinsing of root apex was analyzed without extra preparation for the quantification of Al. In order to minimize sample contamination, all labware were immersed in (20%) HNO_3 followed by rinsing with deionized water.

The crude cell wall and roots were powdered and dry ashed for 5 h at 550 °C to quantify B concentration according to curcumin method by spectrophotometer at 532 nm.

2.5. Fractionation of cell wall components

The sequential extracted crude root cell wall was employed to extract pectin contents colorimetrically (Blumenkrantz and Asboe-Hansen, 1973). The crude cell wall was suspended in 0.05 M acetate buffer at 6.5 pH in 20 mM CDTA (trans-1, 2 diaminocyclohexane-N, N, N', N' tetraacetic acid) with constant stirring ($180 \times g$) overnight at 25 °C. After centrifuging for 12 min at $10000 \times g$. After each centrifugation, the supernatant was collected in tubes and was employed to estimate uronic acid (UA). The standard curve was drawn with galacturonic acid and expressed as galacturonic acid equivalents (GaIA).

Next, the above cell wall pellet was extracted with KOH (24%) in 0.1% NaBH_4 for hemicellulose at 25 °C for 24 h with constant shaking ($180 \times g$). The mixture was centrifuged at $10000 \times g$ for 10 min. The supernatant (mainly hemicellulose) and residues (cellulose) were further processed for measurement of hemicellulose. The total sugars were measured by the Anthrone method while glucose utilized as standard (Yemm and Willis, 1954).

The degree of methyl-esterification was quantified through the method of Anthon and Barrett (2004). The root cell wall was prepared as described above and was saponified with NaOH solution (1.5 M) for 30 min at 25 °C in a water bath and next surplus alkaline was neutralized with H_2SO_4 , and treated with MBTH, Tris-HCl, and alcohol oxidase. Finally, samples were incubated for 20 min at 30 °C. The absorbance was recorded by microplate spectrophotometer at 620 nm.

2.6. Measurement of monoamine oxidase, xanthine, T-AOC and VC concentration

The concentrations of monoamine oxidase (MAO), xanthine oxidase (XOD), total antioxidant capability (T-AOC) and vitamin C (VC) in leaves were measured by commercially available kits, A034, A002, A015 and A009 respectively (Nanjing bio), and procedures were followed by the manufactures guidelines.

2.7. Histochemical analysis of callose deposition and root cell vitality

In order to observe callose, root segments (0–1 cm) were stained with 0.01% aniline blue solution and cross-sectioned root samples were observed by the fluorescence microscope at excitation (460 nm) and emission (390 nm) wavelengths. The double staining with fluorescein diacetate-propidium iodide was used to assess cell viability in the roots tips (0–1 cm) according to Jones and Senft (1985) method at excitation (490 nm) and emission (514 nm) wavelengths.

2.8. Statistical analysis

The data were analyzed with Fisher's analysis of variance "ANOVA" by Statistix 8.1. Treatment means differences were observed by the LSD test at $p < 0.05$. Principle component analysis was carried out by SPSS 20 software.

3. Results

3.1. Effect of boron on the root growth and cell vitality under Al toxicity

Root elongation of trifoliolate seedlings is shown in Fig. 1. Al toxicity with or without B hindered the root elongation, however, such negative effects were more prominent under B_0Al+ . Compared to control treatment, root elongation in B_0Al+ was reduced by 60.75% whilst, B_1Al+ and B_2Al+ treatments exhibited improved root elongation by 95.89% and 105.48% respectively compared to B_0Al+ treatment, indicating a relieve from Al toxicity. The leaf symptom in B_0Al- is considered as boron deficiency, and that in B_0Al+ as boron deficiency together with the Al toxicity (data not shown). The B_1Al+ and B_2Al+ treatments in the absence of Al did not cause any significant effect on the root elongation toxicity, except B deficiency remarkably hampered the growth (Fig. 1).

The root apexes (1 cm) were excised and stained with double staining (fluorescein diacetate-propidium iodide) to envisage Al-

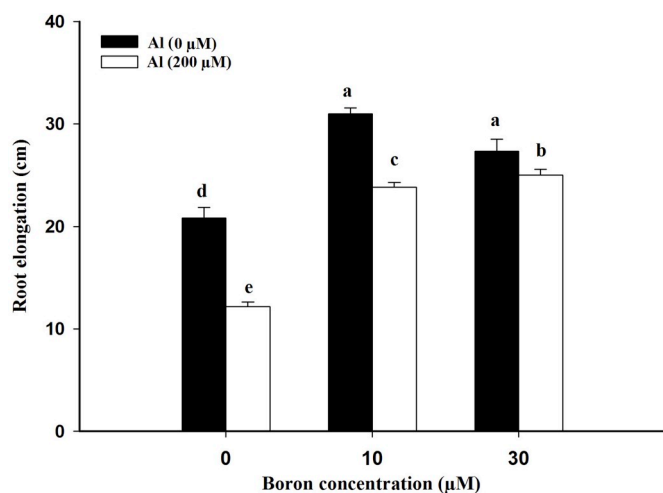


Fig. 1. Total root elongation under different B and Al concentrations. Values are means of three replicates \pm S.E. Columns with different lower case letters are significantly different at ($P < 0.05$).

induced root damage. Images obtained under different B and Al treatments revealed that B_0Al+ and B_0Al- considerably affected cell vitality with root damages (Fig. 2), however, results were more pronounced with B_0Al+ . The treatments of B_1Al+ and B_2Al+ alleviated the Al-induced root damages, with greenish and reduced red patches compared to B_0Al+ . In contrast, the roots exposed to only B without Al exhibited green fluorescence signals behind the root apex.

3.2. Localization of aluminum in the root tips through confocal laser microscope

It was observed that the fluorochrome lumogallion successfully localized the Al ions by confocal laser microscope (CLM) that were strongly bound to apoplast with emitting higher intensities of fluorescence. The cross-sectioned (CS) and longitudinal sections (LS) root portions of B_1Al- and B_2Al- roots in the absence of Al did not stain with lumogallion (data not shown).

The CS root segments detected intense staining and fluorescence signals with B_0Al+ confirmed the increased amount of CW-bound Al outside of the symplast as well as inside cell (Fig. 3). Most of the Al was bound to the apoplast. Same results were also noted in the LS of roots with higher fluorescence signals. On the other hand, the intensities of fluorescence were decreased as the B concentration increased from 10 to 30 μM compared to B_0Al+ treatment, indicating the decreased amount of CW-bound Al. Both CS and LS of root segments displayed homologous results and confirmed reduced accumulation of Al in B treated roots (Fig. 3).

In order to discriminate intracellular nucleus-bound Al, herein, we carried out DAPI staining (blue) and lumogallion (green). The confocal laser micrographs showed that DAPI stained the dsDNA. The images of DAPI were almost spherical, and overlapped images (DAPI + lumogallion) exhibited intracellular nucleus-bound Al under B_0Al+ (Fig. 4). However, the reduced amount of fluorescence channels of Al were detected in B_1Al+ and B_2Al+ irrespective of B concentrations. The images showed a reduced amount of Al in the periphery and interior of the cell. DNA staining with DAPI and lumogallion images confirmed unequivocal reduced adsorbed Al through weak fluorescence compared with B_0Al+ (Fig. 4).

3.3. Fractionation of aluminum

The fractionations of Al in the roots are presented in Table 1. The results indicated enhanced Al accumulation in the cell wall of root apex (0–10 mm) and more than 49.45% of total Al was adsorbed to the CW in B_0Al+ treatment. The citrate washing removed mainly exchangeable Al by 11.63%, 16%, and 24.22% of the corresponding total root tip Al in B_0Al+ , B_1Al+ , and B_2Al+ treatments, respectively (Table 1). On the other hand, B_1Al+ and B_2Al+ treatments exhibited reduced CW-bound Al by 52.24% and 64.60% respectively compared with B_0Al+ treatment.

The B accumulation was significantly increased with increasing B concentration. The Al did not cause any significant effect on B uptake (Table 1).

3.4. Cell wall components

The results indicated that Al toxicity induced high accumulation of pectin and hemicellulose in B_0Al+ treatment and increased by 60.04%, and 149.10% respectively as compared with control treatment (Fig. 5). The B_0Al- also resulted in the increase of pectin predominantly un-methylated pectin and hemicellulose but results were more prominent in the B_0Al+ . On the other hand, the B_1Al+ and B_2Al+ treatments reduced the un-methylation of pectin by 37.05% and 46.78% and hemicellulose by 31.34% and 50% in relation to B_0Al+ treatment respectively (Fig. 5).

The degree of methyl-esterification of pectin defines the extent of

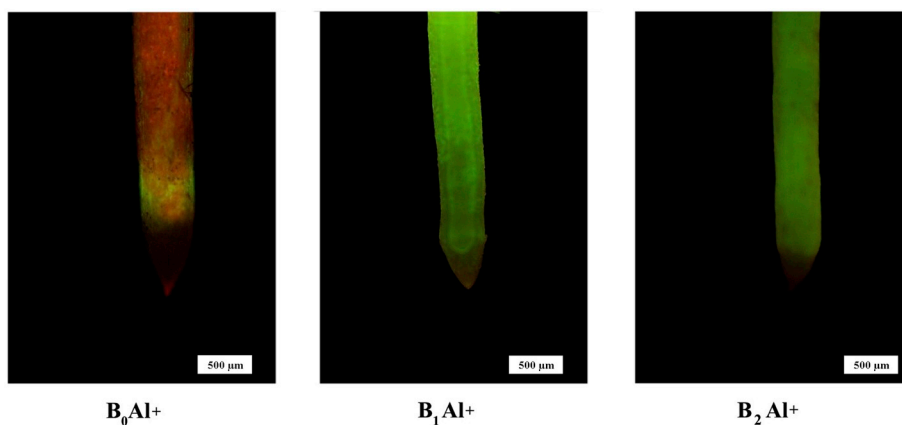


Fig. 2. Fluorescence micrographs of double-stained root tips. Intact cells exhibit green fluorescence due to fluorescein diacetate and propidium iodide emits red fluorescence in damaged cells, Scale bars, 500 µm. (For interpretation of the references to color in this figure legend, the reader is referred to the Web version of this article.)

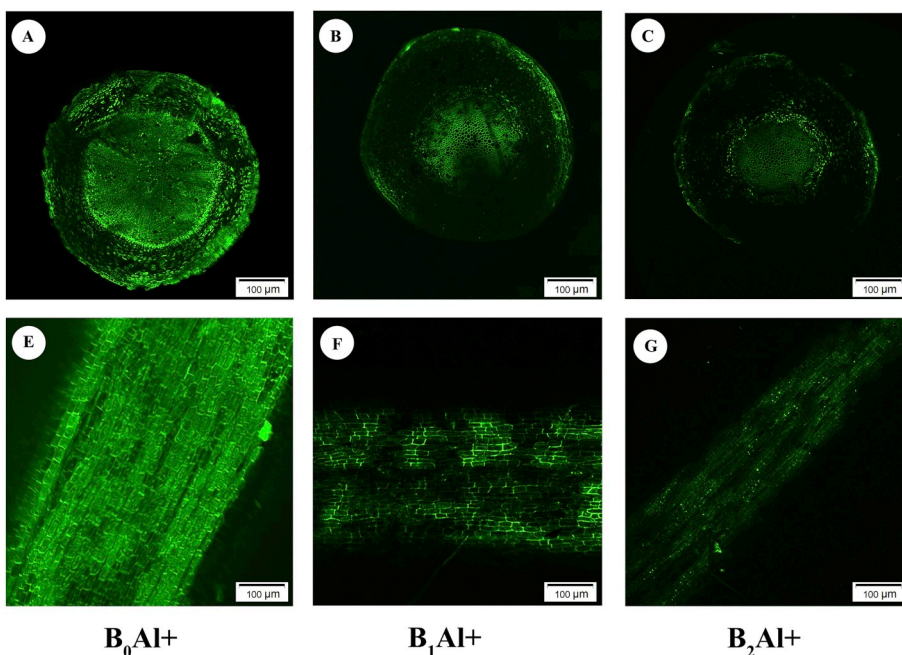


Fig. 3. Aluminum distribution in cross-sections and longitudinal sections of roots exposed to different B and Al concentrations as B₀Al+ (0 µM B + 200 µM Al), B₁Al+ (10 µM B + 200 µM Al) and B₂Al+ (30 µM B + 200 µM Al). Images A, B and C represent the CS sections and D, E and F of longitudinal sections of roots. Lumogallion-Al dye was used to identify the distribution of Al under confocal laser scanning microscopy. Scale bars, 100 µm.

negatively charged sites produced by carboxylic groups on pectin. The extracted cell wall was subjected to the assessment of the degree of methyl-esterification of pectin. The result showed that B₀Al+ remarkably declined the degree of methyl-esterification of pectin compared to the control (Fig. 5). However, the treatments of B₁Al+ and B₂Al+ increased the degree of methyl-esterification by 197.18% and 221.61% respectively with respect to the B₀Al+ treatment, indicating that B supply might regulate the distribution of negatively charged sites on the pectin.

3.5. Activities of monoamine oxidase and xanthine oxidase in leaves

The activities of monoamine oxidase (MAO) and xanthine oxidase (XOD) were greatly affected with aluminum toxicity and deprivation of B (Fig. 6), however, maximum activities were observed with aluminum toxicity especially in B₀Al+ treatment. The aluminum toxicity triggered the activities of MAO and XOD, and significant high concentrations were recorded in the treatment of B₀Al+ and increased by 39.09% and 31.33% compared to control treatment, respectively. However, B₁Al+ and B₂Al+ treatments effectively alleviated the stress by indicating decreased activities of MAO and XOD by 15.69% and 19.76%, compared with B₀Al+, respectively. The activities of MAO and XOD had statistically lower levels than that of B₀Al+ (Fig. 6).

3.6. Vitamin C and total antioxidant capability in leaves

The total antioxidant capability (T-AOC) and vitamin C (VC) in leaves of trifoliate orange was depressed with Al toxicity under B deficiency compared with control treatments. Treatment of B without aluminum had no effect on T-AOC while B deficiency showed an increased level of T-AOC compared with B₀Al+ (Fig. 6). Moreover, compared with B₀Al+, the treatment of B₁Al+ and B₂Al+ indicated an increased T-AOC levels by 100.85% and 155.37%, respectively, indicating that B supply has a significant effect on increasing the total antioxidant capability under Al stress.

3.7. Effect of aluminum on the callose deposition

The induction of callose is considered a chief indicator of Al toxicity and can be deposited within 30 min after Al exposure (Yang et al., 2011a). The results indicated that Al toxicity resulted in the accumulation of the callose (Fig. 7). On the other hand, the roots in the absence of Al displayed reduced induction of callose as indicated by reduced fluorescence. It shows that B supply was found to reduce the callose accumulation.

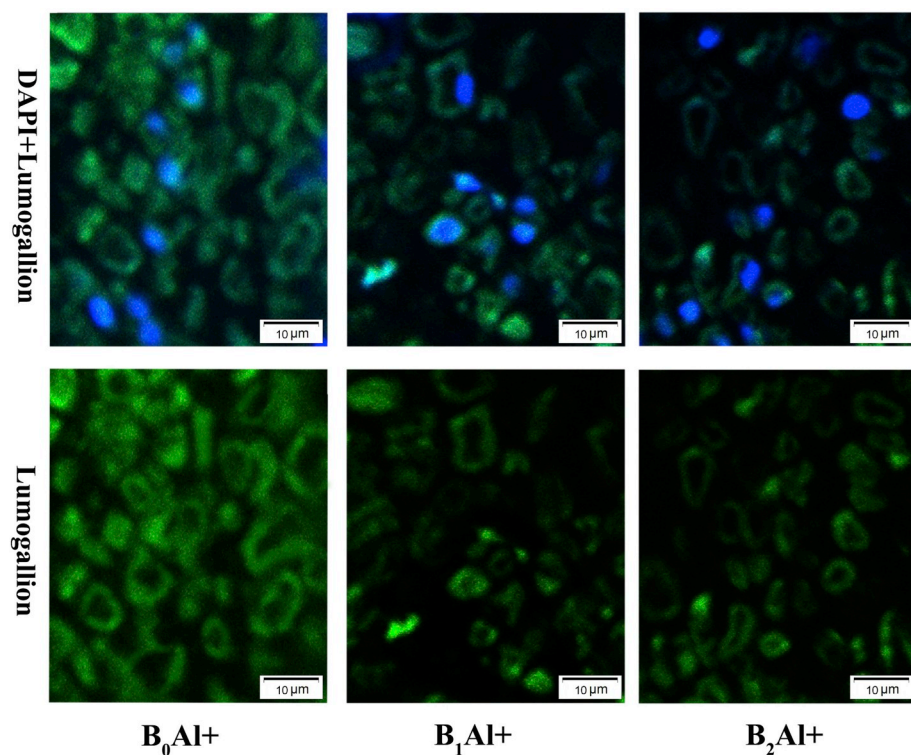


Fig. 4. Confocal fluorescence microscopy images of cells from the meristematic zone of root tips. Where, B_0Al+ (0 μM B + 200 μM Al), B_1Al+ (10 μM B + 200 μM Al) and B_2Al+ (30 μM B + 200 μM Al). (A) Corresponding overlaid with DAPI (B) lumogallion-stained section; note that the lumogallion signal corresponds to the DAPI-stainable part of the nucleus. Scale bars, 10 μm .

3.8. Principal component analysis

The principal component analysis (PCA) of basic factors were analysed to indicate the degree of variation and separation between Al and B treatments. In the absence of Al, B_0 , B_1 , B_2 were separated obviously on PC1 and PC2, and the scores are 83.59% and 14.87%, respectively. The score on PC1 was in the order of $B_0 > B_2 > B_1$, while that on PC2 was $B_2 > B_1 > B_0$. Under three B concentrations, -Al and +Al were significantly separated from PC1 and PC2, and the higher score was obtained in Al-treated plants (Fig. 8), it shows that Al toxicity has an effect on it no matter what concentration of B was applied in the nutrient solution. Under Al stress, B_1 and B_2 were obviously separated from PC1 and PC2, but B_1 and B_2 were not separated from PC1 (Fig. 8), indicating that both appropriate B_1 and high B_2 can alleviate Al toxicity.

4. Discussion

Aluminum toxicity has been well reported to severely affecting the root apex through impeding root elongation (Blamey et al., 1990b; Kochian, 1995). Nevertheless, it is still unclear that interruption of root growth is directly related to the adsorption of Al to the apoplast of root

tip cells (Horst et al., 2010). A number of reports have advocated apoplastic binding of Al as the first target of Al toxicity. The cell wall (CW) is a major pool and exhibits great affinity for Al^{3+} through bearing negative charged carboxylic groups on pectin matrix (Kochian, 1995; Eticha et al., 2005; Horst et al., 2010). For example, *Hordeum vulgare* (barley) roots accumulated 85%–90% of total Al in the CW (Taylor et al., 2000). There is a possibility that Al could interfere multiple processes at the same time that are essential for normal growth of plants (Horst, 1995; Horst et al., 2010; Yang et al., 2011a), therefore interruption of cell process may result in the inhibition of root growth.

Boron has an indispensable role in the development of primary CW and has been reported in the alleviation of Al toxicity in several plants (Yu et al., 2009; Li et al., 2017). The role of B in apoplastic binding and symplastic entry of Al^{3+} is well cleared. The current study was conducted to ascertain the effects of B supply in attenuating CW and nucleus bound Al^{3+} . Highly specific Al dye (lumogallion) and nucleus staining dye (DAPI) were used in the present study. The result showed that B supply improved the total root growth and attenuated the apoplastic bound Al^{3+} . The improved root elongation might be associated with the reduced CW-bound Al.

The plant roots are the most sensitive organs surrounding the toxic rhizosphere and rapidly respond to the unfavorable niches and abiotic

Table 1

Fractionation of B and Al in the roots of trifoliate. Following exposure to Al, root tips (approximately 10 mm) were excised and washed in ice-cold 10 mM citrate. Following the wash, the tips were digested in high-purity HNO_3 for measuring of Al content. The citrate wash was analyzed by the same method without any additional preparation. Total Al concentration is based on the sum of the Al content in the root tips and corresponding citrate wash fraction. Values are means of three replicates \pm S.E. Data of each column indicated with the same letter do not differ significantly at ($P > 0.05$).

Treatments	Boron (mg/g DW)		Aluminum concentrations			
	Roots	Cell wall	Root tips (mg/g)	Citrate wash ($\mu g/g$)	Total Al (mg/g)	Cell Wall (mg/g)
B_0Al-	7.24 \pm 1.14 ^c	5.73 \pm 0.89 ^c	0.28 \pm 0.03 ^d	0.05 \pm 0.01 ^c	0.28 \pm 0.03 ^d	0.12 \pm 0.01d
B_0Al+	8.54 \pm 0.78 ^c	6.14 \pm 0.36 ^c	2.13 \pm 0.11 ^a	280 \pm 21.51 ^b	2.41 \pm 0.07 ^a	1.42 \pm 0.12a
B_1Al-	33.17 \pm 2.06 ^b	19.86 \pm 0.20 ^b	0.24 \pm 0.03 ^d	0.04 \pm 0.01 ^c	0.24 \pm 0.01 ^d	0.12 \pm 0.01d
B_1Al+	31.01 \pm 4.72 ^b	19.45 \pm 1.25 ^b	1.38 \pm 0.07 ^b	274 \pm 12.51 ^b	1.65 \pm 0.06 ^b	0.68 \pm 0.06b
B_2Al-	75.8 \pm 2.86 ^a	44.6 \pm 1.43 ^a	0.21 \pm 0.01 ^d	0.03 \pm 0.02 ^c	0.20 \pm 0.01 ^d	0.09 \pm 0.06d
B_2Al+	74.5 \pm 5.69 ^a	44.8 \pm 2.77 ^a	1.0 \pm 0.03 ^c	312 \pm 13.87 ^a	1.30 \pm 0.02 ^c	0.50 \pm 0.02c

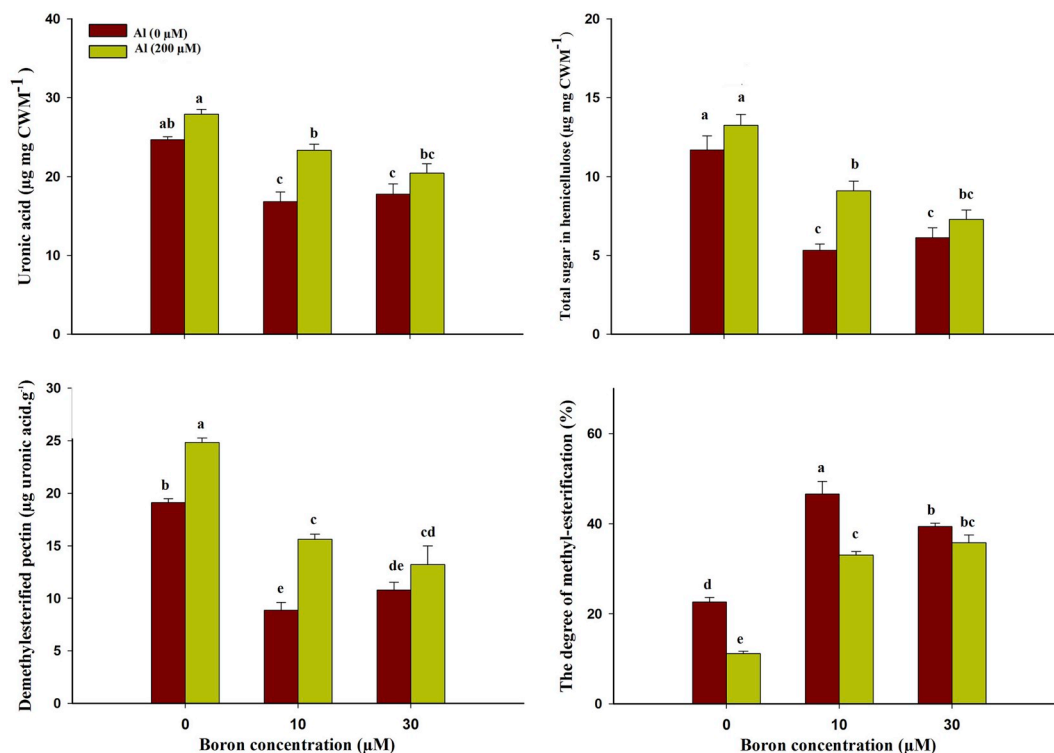


Fig. 5. Fractionation of root cell wall components. Values are means of three replicates ± S.E. Columns with different lower case letters are significantly different at ($P < 0.05$). The demethylesterified pectin content was calculated by the formula of the content of demethylesterified pectin = pectin content × (1-DM/100). The degree of methyl-esterification (DM%) was calculated as mol of methanol per mol of galacturonic acid.

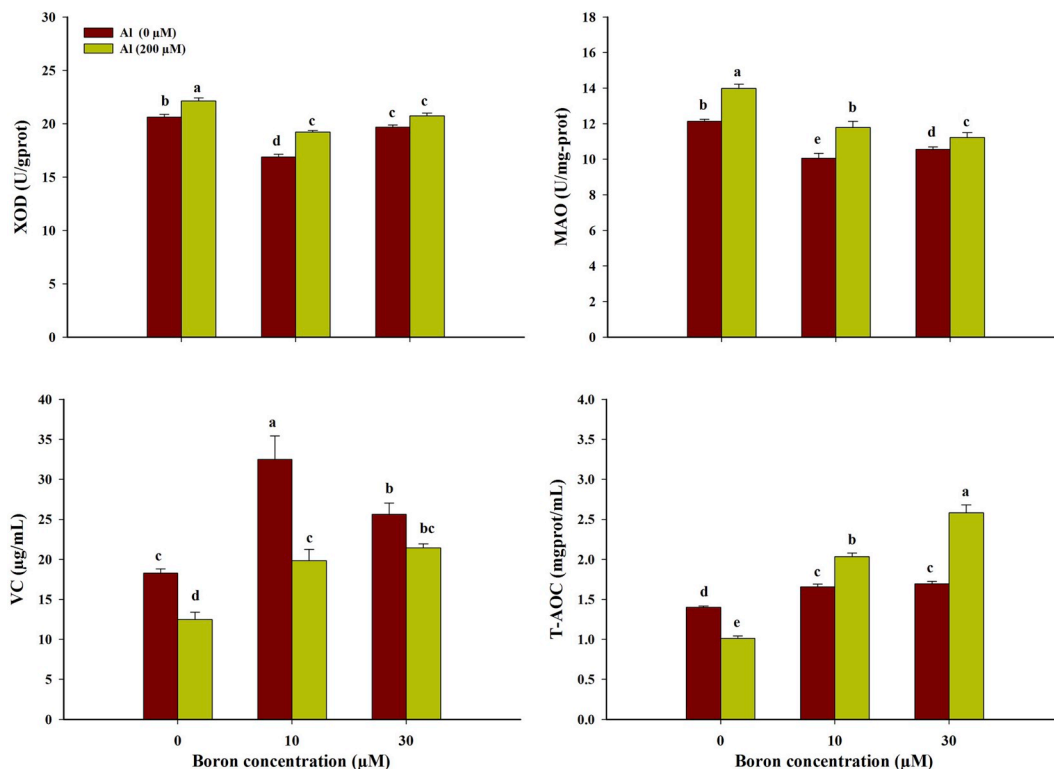


Fig. 6. Activities of MAO, XOD, T-AOC and VC in leaves of trifoliolate. Values are means of three replicates ± S.E. Columns with different lower case letters are significantly different at ($P < 0.05$).

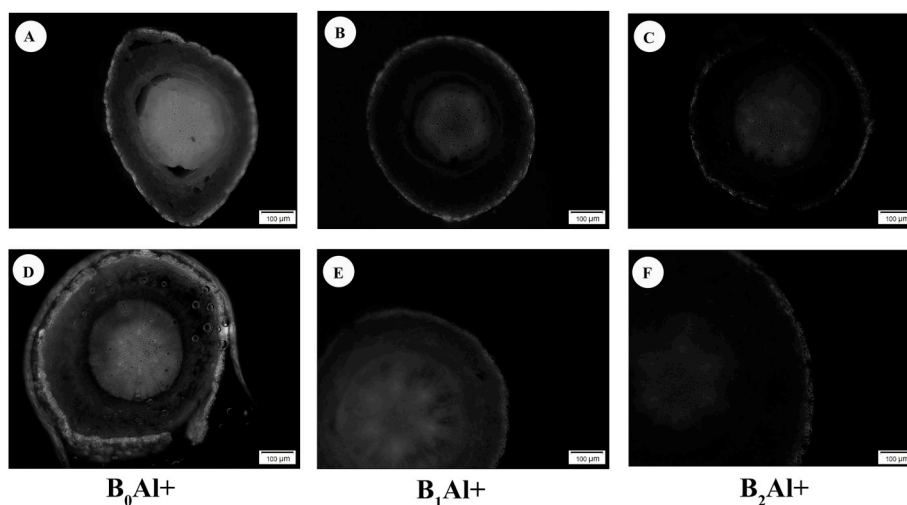


Fig. 7. Influence of B on Al-induced callose synthesis in the roots as B₀Al+ (0 μM B + 200 μM Al), B₁Al+ (10 μM B + 200 μM Al) and B₂Al+ (30 μM B + 200 μM Al). (A, C and B) –overview, focused on the cortex; (C, D and E – close-up view. Scale bars, 100 μm.

stresses including aluminum (Foy, 1992). In the present study, B₀Al+ inhibited the root elongation by 60.75% compared with control (Fig. 1). Cell wall is the first hindrance against toxic elements and provides shielding to the cell organelles (Krzesłowska, 2011). Aluminum quickly binds to the CW and is capable to move into the symplasm and where it likely adheres to the nucleus (Vitorello and Haug, 1996), and ceases mitotic division and interferes with cellular metabolism (Matsumoto, 2000a). It supports the perception that Al toxicity might encourage inhibition of root elongation interfering with nucleus functions. The lumogallion confocal laser microscopy results revealed clear Al³⁺ ions adsorption to the periphery of the CW with higher intensities of fluorescence both in the cross and longitudinal sections of the roots in the B₀Al+ treatment. Moreover, DAPI staining localized the dsDNA with intense blue fluorescence surrounding the green fluorescence (Fig. 4) indicating that Al could enter into cytosol and nucleus could be the target site after apoplast.

Collecting evidence showed that substantial amount of toxic Al resulted in the changes of CW components and might be accountable for changes in normal cell functions (Blamey et al., 1990a; Eticha et al., 2005). The alterations in the CW might restrict the relocation of protein and indispensable ions across the membranes (Baron-Epel et al., 1988),

ultimately affecting CW extensibility. In this experiment, higher accumulations of pectin and hemicellulose could be potential targets of Al toxicity. Several reports suggested that Al preferentially adsorbs to the CW (Yang et al., 2011a). The CEC of CW and carboxylic groups on the pectin matrix particularly de-methyl esterified pectin contributes significantly to the accumulation of Al³⁺ (Delhaize et al., 1993) and might be responsible for impaired root growth (Blamey et al., 1990a; Godbold and Jentschke, 2010). There is a positive relation between root inhibition and CW bound Al; more the CW-Al, the more inhibition of root elongation will be (Eticha et al., 2005).

The B helps in the development of the primary CW and structure by borate cross-linking (Kobayashi et al., 1996; O’neill et al., 2001; O’neill et al., 2004; Kobayashi et al., 2017). The primary CW ensures intercellular communication and transportation of signals across the membrane (Knox, 2008). The CW bears changes in the atmosphere. Boron tightly holds the polysaccharides together and defines a stable CW with optimized pores. The organized cross-linked network of CW components might restrict the entry of toxic molecules including Al (Fleischer et al., 1999; Corrales et al., 2008; Riaz et al., 2018a). In the present study, B supply decreased the uptake of Al³⁺ both in the CW and in the root segments. Apart from the pectin, hemicellulose also contributes to

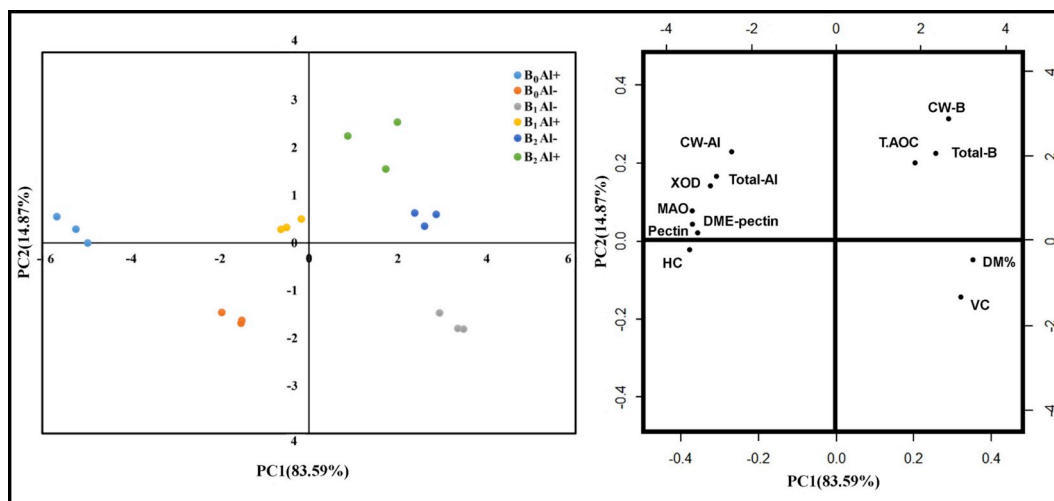


Fig. 8. Principle component analysis of essential plant measured factors. The PCA separated the B₀Al+ and B treated plants under aluminum toxicity on PC1 and PC2 accounting for 71% and 15.8% respectively of the total variation. PCA also clearly isolated essential factors on the PC1 and PC2. Whereas B₀Al- (0 μM B + 0 μM Al), B₀Al+ (0 μM B + 200 μM Al), B₁Al- (10 μM B + 0 μM Al), B₁Al+ (10 μM B + 200 μM Al), B₂Al- (30 μM B + 0 μM Al), and B₂Al+ (30 μM B + 200 μM Al).

the accumulation of Al (Yang et al., 2011a). The results showed that B supply tended to increase the hemicellulose of the CW and this, in turn, reduced the adsorption of Al to hemicellulose. Boron tolerance to Al toxicity might be related to reduced alterations in the CW components (Stass et al., 2007; Li et al., 2017). The accumulation of hemicellulose in the B₀Al + treatments indicated that Al toxicity stimulated biosynthesis of hemicellulose to overcome the stress. On the other hand, the CW of B treated roots demonstrated a relatively lower accumulation of hemicellulose. The polysaccharides regulate the mechanical extensibility of the CW, therefore, hemicellulose might trigger increase of CW thickness which ultimately might decrease the extensibility of the CW (Sakurai, 1991; Kobayashi et al., 2017), leading to the rigidity and stiffness as well as damage of plasticity of CW (Heidarabadi et al., 2011).

The plant defensive system plays an important part against metal-induced oxidative damages produced by over-accumulation of reactive oxygen species (ROS). In the normal plant system, reactive oxygen species are produced during plant metabolism mechanism and there is always a balance between ROS and ROS-scavenging antioxidant enzymes (Hussain et al., 2016; Yan et al., 2018a,b). However, due to stress conditions of metal toxicity including aluminum, ROS are accumulated and may induce oxidative stress if they are not scavenged by ROS scavengers which ultimately results in oxidative damages in plants even can induce root injuries and cell death (Riaz et al., 2018) which could be directly related to inhibition of root elongation. Results showed that B supply to seedlings reduced the aluminum-induced root injuries by maintaining total enzyme activities, However, Al reduced the total enzyme activities without B (Fig. 6).

Aluminum is not a transitional metal and it itself does not induce redox reaction, however, it is able to induce oxidative damages and tempts cellular injuries (Matsumoto, 2000a; Yamamoto et al., 2002, 2003; Riaz et al., 2018b). On the other hand, the induction of callose in the roots has been extensively used as a marker of aluminum toxicity (Yang et al., 2011b). Aluminum has a great affinity for negatively charged sites than Ca²⁺ does, and aluminum displaces other cations. The interactions with the membrane constituents induce a modification of membrane fluidity and membrane permeability (Khan et al., 2009). It has been reported that structural changes in the plasma membrane are associated with the induction of callose and disturbance in the cytosolic Ca²⁺ gradient. The surface contact of aluminum with plasma membrane changes the negativity of the membrane and causes the depolarization of the membranes (Kinraide et al., 1992; Sivaguru and Horst, 1998). The reason for alterations in the negativity and depolarization might be due to disturbance of H⁺ homeostasis in the cytosol through the inhibition of H⁺-ATPase activities which ultimately affect and interrupt the transports of ions by changes the plasma membrane characteristics (Plieth et al., 1999; Ahn et al., 2001). The dislocation of membrane cations by aluminum induces the formation of callose (β-1, 3-glucane) as a result of β-1, 3-glucanase synthetase (Gupta et al., 2013). The displacement of Ca²⁺ may worsen the apoplast Ca²⁺ pool necessary to activate callose induction (Ryan et al., 1992; Gupta et al., 2013). Callose is synthesized on the plasma membrane and activated by increased concentration of Ca²⁺ ions in the cytoplasm. Thus, the callose induction is a critical marker of aluminum toxicity and can be induced at low concentration of aluminum. Callose might move from the plasma membrane to apoplast that further inhibits the essential nutrients uptake and water from the surroundings (Matsumoto, 2000b; Sivaguru et al., 2000; Yamamoto et al., 2003) and induces reactive oxygen species. The results demonstrated that Al toxicity accumulated a substantial amount of callose in B₀Al +. It was noted that in the absence of Al treatment, the roots had no effect on callose induction irrespective of B treatments (data not shown). B supply remarkably tended to decrease the callose formation and results were more prominent with B₂Al +. Jones et al. (2006) determined the spatial and temporal coordination of aluminum movement in the maize roots and its corresponding induction of callose by employing morin staining in the root apex and proposed that there exists a close spatial and temporal dynamics; callose

induction is largely dependent on the accumulation of aluminum in the roots. After 24 h of aluminum exposure, the center of roots was found to be occupied by aluminum and induced substantial changes in the root morphology. Aluminum toxicity not only induced callose induction but also accumulated ROS in the root zone which ultimately resulted in the rigidity of the CW and suggested that ROS and Ca²⁺ might play a role in the signal transduction that clues to the induction of callose and subsequent apoptosis of the epidermal sheets. Our findings are in accordance with Yu et al. (2009) that B supply positively protects roots from toxic Al and subsequently reduces callose induction.

5. Conclusion

The study results reinforce the view that apoplast could be target site of Al accumulations which eventually demonstrated inhibited root growth. The increased amount of CW-bound Al was clearly detected with lumogallion and DAPI in the treatment of B₀Al + by confocal laser microscopy. On the other hand, B supply reduced the changes in the cell wall components by decreasing pectin and hemicellulose; a possible ligand for Al adsorption. The B supply reduced the apoplast Al³⁺, callose deposition and improved total root elongation and cell vitality. The results imply that B due to its role in the cell wall formation could protect roots against toxic Al³⁺ by attenuating apoplastic binding of Al³⁺ in trifoliate orange.

Contributions

M.R and C.J designed and supervised this study; M. R conducted the experiments, performed data interpretation, and drafted the manuscript; X, W helped in determining cell wall components; LY, and A.O helped in replacing nutrition solution in the experiment and determining B and Al concentration; S.H helped to revise the manuscript grammatically. All authors read and approved the final manuscript.

Funding

This work was supported by the National Natural Science Foundation of China, 2017PY055 This work was supported by the National Natural Science Foundation of China (41271320) and the Fundamental Research Funds for the Central Universities (2017PY055).

References

- Ahn, S.J., Sivaguru, M., Osawa, H., Chung, G.C., Matsumoto, H., 2001. Aluminum inhibits the H⁺-ATPase activity by permanently altering the plasma membrane surface potentials in squash roots. *Plant Physiol.* 126, 1381.
- Alva, A., Asher, C., Edwards, D., 1986. The role of calcium in alleviating aluminium toxicity. *Aust. J. Agric. Res.* 37, 375–382.
- Anthon, G.E., Barrett, D.M., 2004. Comparison of three colorimetric reagents in the determination of methanol with alcohol oxidase. Application to the assay of pectin methylesterase. *J. Agric. Food Chem.* 52, 3749–3753.
- Baron-Epel, O., Gharyal, P.K., Schindler, M., 1988. Pectins as mediators of wall porosity in soybean cells. *Planta* 175, 389–395.
- Blamey, F., Edmeades, D., Wheeler, D., 1990a. Role of root cation-exchange capacity in differential aluminum tolerance of Lotus species. *J. Plant Nutr.* 13, 729–744.
- Blamey, F.P.C., Edmeades, D.C., Wheeler, D.M., 1990b. Role of root cation-exchange capacity in differential aluminum tolerance of lotus species. *J. Plant Nutr.* 13, 729–744.
- Blumenkrantz, N., Asboe-Hansen, G., 1973. New method for quantitative determination of uronic acids. *Anal. Biochem.* 54, 484–489.
- Chang, Y.C., Yamamoto, Y., Matsumoto, H., 1999. Accumulation of aluminum in the cell wall pectin in cultured tobacco (*Nicotiana tabacum* L.) cells treated with a combination of aluminum and iron. *Plant Cell Environ.* 22, 1009–1017.
- Corrales, I., Poschenrieder, C., Barceló, J., 2008. Boron-induced amelioration of aluminum toxicity in a monocot and a dicot species. *J. Plant Physiol.* 165, 504–513.
- Delhaize, E., Craig, S., Beaton, C.D., Bennet, R.J., Jagadish, V.C., Randall, P.J., 1993. Aluminum tolerance in wheat (*Triticum aestivum* L.) (I. Uptake and distribution of aluminum in root apices). *Plant Physiol.* 103, 685–693.
- Eticha, D., Stass, A., Horst, W.J., 2005. Cell-wall pectin and its degree of methylation in the maize root-apex: significance for genotypic differences in aluminium resistance. *Plant Cell Environ.* 28, 1410–1420.
- Fleischer, A., O'Neill, M.A., Ehwald, R., 1999. The pore size of non-graminaceous plant

- cell walls is rapidly decreased by borate ester cross-linking of the pectic polysaccharide rhamnogalacturonan II. *Plant Physiol.* 121, 829–838.
- Foy, C.D., 1992. Soil chemical factors limiting plant root growth. In: *Limitations to Plant Root Growth*. Springer, pp. 97–149.
- Godbold, D.L., Jentschke, G., 2010. Aluminum accumulation in root cell walls coincides with inhibition of root growth but not with inhibition of magnesium uptake in Norway spruce. *Physiol. Plantarum* 102, 553–560.
- Gupta, N., Gaurav, S.S., Kumar, A., 2013. Molecular basis of aluminium toxicity in plants: a review. *Am. J. Plant Sci.* 4, 21–37.
- Han, S., Chen, L.-S., Jiang, H.-X., Smith, B.R., Yang, L.-T., Xie, C.-Y., 2008. Boron deficiency decreases growth and photosynthesis, and increases starch and hexoses in leaves of citrus seedlings. *J. Plant Physiol.* 165, 1331–1341.
- Heidarabadi, M.D., Ghanati, F., Fujiwara, T., 2011. Interaction between boron and aluminium and their effects on phenolic metabolism of *Linum usitatissimum* L. roots. *Plant Physiol. Biochem.* 49, 1377–1383.
- Horst, W.J., 1995. The role of the apoplast in aluminium toxicity and resistance of higher plants: a review. *J. Plant Nutr.* Soil Sci. 158, 419–428.
- Horst, W.J., Wang, Y., Eticha, D., 2010. The role of the root apoplast in aluminium-induced inhibition of root elongation and in aluminium resistance of plants: a review. *Ann. Bot.* 106, 185–197.
- Hussain, S., Khan, F., Cao, W., Wu, L., Geng, M., 2016. Seed priming alters the production and detoxification of reactive oxygen intermediates in rice seedlings grown under sub-optimal temperature and nutrient supply. *Front. Plant Sci.* 7, 439.
- Jones, K.H., Senft, J.A., 1985. An improved method to determine cell viability by simultaneous staining with fluorescein diacetate-propidium iodide. *J. Histochem. Cytochem.* 33, 77–79.
- Jones, D., Blancaflor, E., Kochian, L., Gilroy, S., 2006. Spatial coordination of aluminium uptake, production of reactive oxygen species, callose production and wall rigidification in maize roots. *Plant Cell Environ.* 29, 1309–1318.
- Khan, M.S., Tawarayama, K., Sekimoto, H., Koyama, H., Kobayashi, Y., Murayama, T., Chuba, M., Kambayashi, M., Shiono, Y., Uemura, M., 2009. Relative abundance of Delta(5)-sterols in plasma membrane lipids of root-tip cells correlates with aluminium tolerance of rice. *Physiol. Plantarum* 135, 73–83.
- Kinraide, T.B., Ryan, P.R., Kochian, L.V., 1992. Interactive effects of Al₃, H⁺, and other cations on root elongation considered in terms of cell-surface electrical potential. *Plant Physiol.* 99, 1461–1468.
- Knox, J.P., 2008. Revealing the structural and functional diversity of plant cell walls. *Curr. Opin. Plant Biol.* 11, 308–313.
- Kobayashi, M., Matoh, T., Azuma, J., 1996. Two chains of rhamnogalacturonan II are cross-linked by borate-diol ester bonds in higher plant cell walls. *Plant Physiol.* 110, 1017–1020.
- Kobayashi, M., Miyamoto, M., Matoh, T., Kitajima, S., Hanano, S., Sumerta, I.N., Narise, T., Suzuki, H., Sakurai, N., Shibata, D., 2017. Mechanism underlying rapid responses to boron deprivation in *Arabidopsis* roots. *Soil Sci. Plant Nutr.* 1–10.
- Kochian, L.V., 1995. Cellular mechanisms of aluminum toxicity and resistance in plants. *Annu. Rev. Plant Biol.* 46, 237–260.
- Kochian, L.V., Hoekenga, O.A., Pineros, M.A., 2004. How do crop plants tolerate acid soils? Mechanisms of aluminum tolerance and phosphorous efficiency. *Annu. Rev. Plant Biol.* 55, 459–493.
- Kollmeier, M., Felle, H.H., Horst, W.J., 2000. Genotypical differences in aluminum resistance of maize are expressed in the distal part of the transition zone. Is reduced basipetal auxin flow involved in inhibition of root elongation by aluminum? *Plant Physiol.* 122, 945–956.
- Krzyszowska, M., 2011. The cell wall in plant cell response to trace metals: polysaccharide remodeling and its role in defense strategy. *Acta Physiol. Plant.* 33, 35–51.
- Lazof, D.B., Holland, M.J., 1999. Evaluation of the aluminium-induced root growth inhibition in isolation from low pH effects in *Glycine max*, *Pisum sativum* and *Phaseolus vulgaris*. *Funct. Plant Biol.* 26, 147–157.
- Lenoble, M., Blevins, D., Miles, R., 1996a. Prevention of aluminium toxicity with supplemental boron. II. Stimulation of root growth in an acidic, high-aluminium subsoil. *Plant Cell Environ.* 19, 1143–1148.
- Lenoble, M., Blevins, D., Sharp, R., Cumbie, B., 1996b. Prevention of aluminium toxicity with supplemental boron. I. Maintenance of root elongation and cellular structure. *Plant Cell Environ.* 19, 1132–1142.
- Li, X.W., Liu, J.Y., Fang, J., 2017. Boron supply enhances aluminum tolerance in root border cells of pea (*Pisum sativum*) by interacting with cell wall pectins. *Front. Plant Sci.* 8.
- Llugany, M., Poschenrieder, C., Barceló, J., 1995. Monitoring of aluminium-induced inhibition of root elongation in four maize cultivars differing in tolerance to aluminium and proton toxicity. *Physiol. Plantarum* 93, 265–271.
- Loomis, W.D., Durst, R., 1992. Chemistry and biology of boron. *Biofactors* 3, 229–239.
- Ma, J.F., Shen, R., Nagao, S., Tanimoto, E., 2004. Aluminum targets elongating cells by reducing cell wall extensibility in wheat roots. *Plant Cell Physiol.* 45, 583–589.
- Matsumoto, H., 2000a. Cell Biology of Aluminium Toxicity and Tolerance in Higher Plants.
- Matsumoto, H., 2000b. Cell biology of aluminum toxicity tolerance in higher plants. *Int. Rev. Cytol.* 200, 1–46.
- O'Neill, M.A., Eberhard, S., Albersheim, P., Darvill, A.G., 2001. Requirement of borate cross-linking of cell wall rhamnogalacturonan II for *Arabidopsis* growth. *Science* 294, 846–849.
- O'Neill, M.A., Ishii, T., Albersheim, P., Darvill, A.G., 2004. Rhamnogalacturonan II: structure and function of a borate cross-linked cell wall pectic polysaccharide. *Annu. Rev. Plant Biol.* 55, 109–139.
- Plieth, C., Sattelmacher, B., Hansen, U.P., Knight, M.R., 1999. Low-pH-mediated elevations in cytosolic calcium are inhibited by aluminium: a potential mechanism for aluminium toxicity. *Plant J.* 18, 643–650.
- Poschenrieder, C., Gunesé, B., Corrales, I., Barceló, J., 2008. A glance into aluminium toxicity and resistance in plants. *Sci. Total Environ.* 400, 356–368.
- Riaz, M., Yan, L., Wu, X., Hussain, S., Aziz, O., Imran, M., Rana, M.S., Jiang, C., 2018a. Boron reduces aluminum-induced growth inhibition, oxidative damage and alterations in the cell wall components in the roots of trifoliolate orange. *Ecotoxicol. Environ. Saf.* 153, 107–115.
- Riaz, M., Yan, L., Wu, X., Hussain, S., Aziz, O., Wang, Y., Imran, M., Jiang, C., 2018b. Boron alleviates the aluminum toxicity in trifoliolate orange by regulating antioxidant defense system and reducing root cell injury. *J. Environ. Manag.* 208, 149–158.
- Ryan, P.R., Shaff, J.E., Kochian, L.V., 1992. Aluminum toxicity in roots correlation among ionic currents, ion fluxes, and root elongation in aluminium-sensitive and aluminium-tolerant wheat cultivars. *Plant Physiol.* 99, 1193–1200.
- Sakurai, N., 1991. Cell wall functions in growth and development—a physical and chemical point of view. *Bot. Mag.* = *Shokubutsu-gaku-zasshi* 104, 235–251.
- Silva, I.R., Smyth, T.J., Moxley, D.F., Carter, T.E., Allen, N.S., Ruffy, T.W., 2000. Aluminum accumulation at nuclei of cells in the root tip. Fluorescence detection using lumogallion and confocal laser scanning microscopy. *Plant Physiol.* 123, 543–552.
- Sivaguru, M., Fujiwara, T., Samaj, J., Baluska, F., Yang, Z., Osawa, H., Maeda, T., Mori, T., Volkmann, D., Matsumoto, H., 2000. Aluminium-induced 1→3-β-D-Glucan inhibits cell-to-cell trafficking of molecules through plasmodesmata. A new mechanism of aluminum toxicity in plants. *Plant Physiol.* 124, 991–1006.
- Sivaguru, M., Horst, W.J., 1998. The distal part of the transition zone is the most aluminium-sensitive apical root zone of maize. *Plant Physiol.* 116, 155–163.
- Stass, A., Kotur, Z., Horst, W.J., 2007. Effect of boron on the expression of aluminium toxicity in *Phaseolus vulgaris*. *Physiol. Plantarum* 131, 283–290.
- Taylor, G.J., McDonald-Stephens, J.L., Hunter, D.B., Bertsch, P.M., Elmore, D., Rengel, Z., Reid, R.J., 2000. Direct measurement of aluminum uptake and distribution in single cells of chara corallina. *Plant Physiol.* 123, 987–996.
- Tice, K.R., Parker, D.R., Demason, D.A., 1992. Operationally defined apoplastic and symplastic aluminum fractions in root tips of aluminum-intoxicated wheat. *Plant Physiol.* 100, 309–318.
- Uexküll, H.R.V., Mutert, E., 1995. Global extent, development and economic impact of acid soils. *Plant Soil* 171, 1–15.
- Vitorello, V.A., Haug, A., 1996. Short-term aluminium uptake by tobacco cells - growth dependence and evidence for internalization in a discrete peripheral region. *Physiol. Plantarum* 97, 536–544.
- Wu, X., Riaz, M., Yan, L., Du, C., Liu, Y., Jiang, C., 2017. Boron deficiency in trifoliolate orange induces changes in pectin composition and architecture of components in root cell walls. *Front. Plant Sci.* 8.
- Yamamoto, Y., Kobayashi, Y., Devi, S.R., Rikiishi, S., Matsumoto, H., 2002. Aluminum toxicity is associated with mitochondrial dysfunction and the production of reactive oxygen species in plant cells. *Plant Physiol.* 128, 63–72.
- Yamamoto, Y., Kobayashi, Y., Devi, S.R., Rikiishi, S., Matsumoto, H., 2003. Oxidative stress triggered by aluminum in plant roots. In: *Roots: the Dynamic Interface between Plants and the Earth*. Springer, pp. 239–243.
- Yan, L., Riaz, M., Wu, X., Wang, Y., Du, C., Jiang, C., 2018a. Interaction of boron and aluminum on the physiological characteristics of rape (*Brassica napus* L.) seedlings. *Acta Physiol. Plant.* 40, 33.
- Yan, L., Riaz, M., Muhammad, W., X.W., Du, C.Q., Liu, Y.L., Lv, B., Jiang, C.C., 2018b. Boron inhibits aluminum-induced toxicity to citrus by stimulating antioxidant enzyme seedlings. *J. Environ. Sci. Health Part C* 36 (3), 145–163.
- Yang, J.L., Zhu, X.F., Peng, Y.X., Zheng, C., Li, G.X., Liu, Y., Shi, Y.Z., Zheng, S.J., 2011a. Cell wall hemicellulose contributes significantly to aluminum adsorption and root growth in *Arabidopsis*. *Plant Physiol.* 155, 1885–1892.
- Yang, L.-T., Jiang, H.-X., Tang, N., Chen, L.-S., 2011b. Mechanisms of aluminum-tolerance in two species of citrus: secretion of organic acid anions and immobilization of aluminum by phosphorus in roots. *Plant Sci.* 180, 521–530.
- Yemm, E.W., Willis, A.J., 1954. The estimation of carbohydrates in plant extracts by anthrone. *Biochem. J.* 57, 508.
- Yu, M., Shen, R., Xiao, H., Xu, M., Wang, H., Wang, H., Zeng, Q., Bian, J., 2009. Boron alleviates aluminum toxicity in pea (*Pisum sativum*). *Plant Soil* 314, 87.